J Therm Anal Calorim (2010) 100:623–627
DOI 10.1007/s10973-009-0416-6

Thermal decomposition mechanism and quantum chemical investigation of hydrazine 3-nitro-1,2,4-triazol-5-one (HNTO)

Jian-Hua Yi · Feng-Qi Zhao · Ying-Hui Ren · Si-Yu Xu · Hai-Xia Ma · Rong-Zu Hu

Received: 29 March 2009 / Accepted: 12 August 2009 / Published online: 27 October 2009

Abstract The thermal decomposition mechanism of hydrazine 3-nitro-1,2,4-triazol-5-one (HNTO) compound was studied by means of differential scanning calorimetry (DSC), thermogravimetry and derivative thermogravimetry (TG-DTG), and the coupled simultaneous techniques of in situ thermolysis cell with rapid scan Fourier transform infrared spectroscopy (in situ thermolysis/RSFTIR). The thermal decomposition mechanism is proposed. The quantum chemical calculation on HNTO was carried out at B3LYP level with 6-31G+(d) basis set. The results show that HNTO has two exothermic decomposition reaction stages: nitryl group break first away from HNTO molecule, then hydrazine group break almost simultaneously away with carbonyl group, accompanying azole ring breaking in the first stage, and the reciprocity of fragments generated from the decomposition reaction is appeared in the second one. The C–N bond strength sequence in the pentabasic ring (shown in Scheme 1) can be obtained from the quantum chemical calculation as: C3–N4 > N2–C3 > N4–C5 > N1–C5. The weakest bond in NTO^- is N7–C3. N11–N4 bond strength is almost equal to N4–C5. The theoretic calculation is in agreement with that of the thermal decomposition experiment.

J.-H. Yi · F.-Q. Zhao (✉) · S.-Y. Xu · R.-Z. Hu
Xi'an Modern Chemistry Research Institute, Xi'an 710065, China
e-mail: npecc@21cn.com

Y.-H. Ren · H.-X. Ma
School of Chemical Engineering, Northwest University, Xi'an 710069, China

Y.-H. Ren
e-mail: yiren@nwu.edu.cn

Keywords Hydrazine 3-nitro-1,2,4-triazol-5-one (HNTO) · Quantum chemical calculation · Thermal decomposition mechanism

Introduction

3-Nitro-1,2,4-triazol-5-one (NTO) has a acidic nature (pKa = 3.67), and it can form metal salts and amine salts with aromatic and aliphatic amines, lots of metal salts and amine salts of NTO have been reported [1–21]. Hydrazine 3-nitro-1,2,4-triazol-5-one (HNTO) compound prepared by the reaction of NTO with hydrazine hydrate has lower acidity and higher nitrogen content than NTO, and it possess a higher chemical stability and consistency in propellant and explosive formulations. The preparation, characterization, and non-isothermal reaction kinetics of HNTO have been reported in [22]. In this article, the thermal decomposition mechanism of HNTO was studied by means of differential scanning calorimetry (DSC), thermogravimetry and derivative thermogravimetry (TG-DTG), and the coupled simultaneous techniques of in situ thermolysis cell with rapid scan Fourier transform infrared spectroscopy (in situ thermolysis/RSFTIR), and the population analysis and stability of HNTO were investigated through the theoretical calculation.

Experimental

Materials

HNTO used in this research was prepared according to [22]. Elemental anal. (%) calcd. for $C_2N_6H_6O_3$: C 14.81, H 3.70, N 51.83, O 29.62; found: C 15.02, H 3.75, N 51.51, O

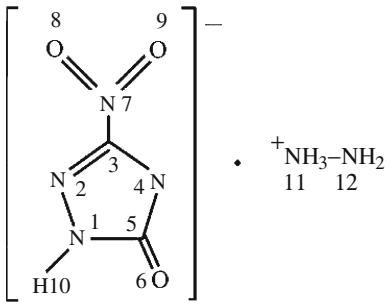

Scheme 1 Scheme of HNTO

29.33. XRD [2θ (°), I/I_0 (%)]: 13.30, 60; 14.20, 58; 16.24, 45; 22.38, 100; 26.30, 48; 27.72, 48; 35.62, 21. ^{13}C-NMR(500 MHz, ppm): δ (C=O), 164.6; δ(C–NO_2), 159.3. ^{15}N-NMR(500 MHz, ppm): δ(–NO_2) 361.1; δ[N(2)], 268.2; δ[N(1)], 192.8; δ[N(4)], 182.7; δ(–NH_2), 49.3. The scheme of HNTO is shown in Scheme 1.

Thermal analysis [23–25]

DSC and TG-DTG curves under the condition of flowing nitrogen gas (purity, 99.999%; flowing rate, 60 cm^3 min^{-1}; 0.1 MPa) were obtained by using a TA 910S differential scanning calorimeter (TA Co., USA) and a TA2950 thermal analyzer (TA Co., USA), respectively. Sample mass, about 0.5 mg, heating rate, 10 °C min^{-1}, reference sample, α-Al_2O_3, type of crucible, aluminum pan with a pierced lid. The coupled simultaneous techniques of in situ thermolysis cell (Amoy University Instrument Co., China) with rapid scan Fourier transform infrared spectroscopy (Nicolet 60SXR, Nicolet Co., USA) were employed to explore the thermal decomposition mechanism. The cell heating rate, 10 °C min^{-1}, atmosphere, air. Solid thermolysis spectra acquisition rate, 7.48 files min^{-1}, resolution, 4 cm^{-1}, a DTGS detector.

Model and method for quantum chemical calculation

A unit of the structure, whose energy is minimized with MOPAC method in Chem3D, was selected as the initial structure, and B3LYP/6-31+G(d) method in Gaussian 03 package was used to optimize the structure of the title compound and compute its frequencies [26]. Vibration analysis showed that the optimized structure is in accordance with the minimum points on the potential energy planes, which means no virtual frequencies, proving that the obtained optimized structure is stable. All the convergent precisions were the system default values, and all the calculations were carried out on the IBM computer.

Results and discussion

DSC and TG-DTG analysis

The DSC and TG-DTG curves of HNTO at the pressure of 0.1 MPa are shown in Figs. 1 and 2. The DSC curve consists of two exothermic peaks, corresponding to two mass loss stages in TG curve and two apparent peaks in DTG curve. The sharp exothermic peak at temperatures between 184.90 and 218.10 °C, corresponding to the main exothermic decomposition process (stage I) of HNTO with mass loss 45.62%, onset temperature (T_e) at 208.50 °C, and summit peak (T_p) at 210.70 °C, which is lower than that of NTO at 272.80 °C and RDX at 238.90 °C, and this is because of the missing active hydrogen of NTO and the different decomposition mechanism between HNTO and NTO.

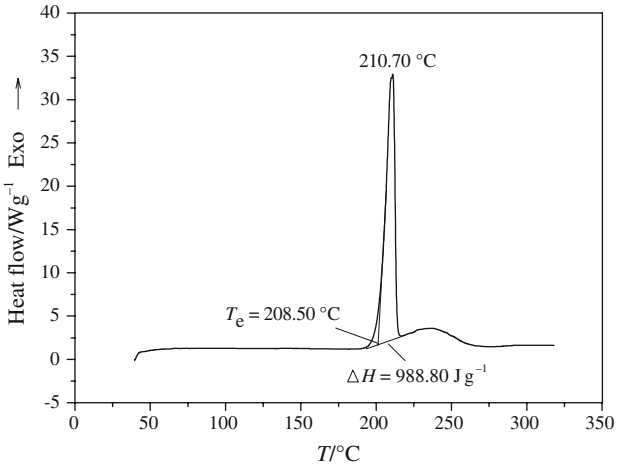

Fig. 1 DSC curve of HNTO (β = 10 °C min^{-1})

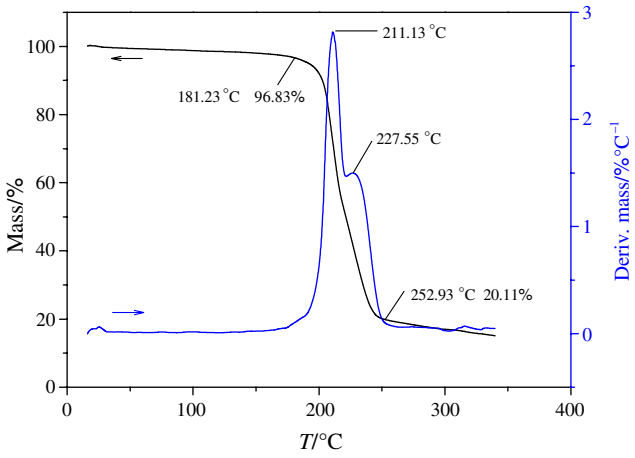

Fig. 2 TG-DTG curve of HNTO (β = 10 °C min^{-1})

Thermolysis in the heated IR cell

Thermolysis/RSFTIR was used to analyze the condensed phase products of the thermal decomposition of HNTO under the linear temperature rise condition in real time.

The RSFTIR spectrum of HNTO at room temperature (25 °C) is shown in Fig. 3. ν[N(4)–NH], 3350.05 cm^{-1} and 3283.89 cm^{-1}; ν(C–NH), 2735.14 cm^{-1}; ν(C=O), 1696 cm^{-1}; ν_{as} (C–NO_2), 1509.19 cm^{-1}; ν_s (C–NO_2), 1318.49 cm^{-1}.

The IR absorption spectra of the condensed phase thermolysis products at various temperatures and the curves of characteristic bands intensity changing with temperature are shown in Figs. 4 and 5, respectively. It can be clearly seen that the band intensity of nitryl (Fig. 5b, c) and carbonyl (Fig. 5a) is weakened first when HNTO is heated to a certain temperature, making great changes of the spectra intensity of –NH (Fig. 5d, e) derived from hydrazine group occur: the spectra intensity ascends up to the maximum value at 190 °C from original 137 °C and almost minimized to zero at 240–250 °C. The reason may be that the break of carbonyl and nitryl away from HNTO body, making the spectra intensity of N(4)–NH increase. At the same time, N(4)–NH breaks with the temperature rising, and let the gaseous nitrogen compounds get away from the condensed phase. In the process, –CN and –OCN spectra intensities (Fig. 5f, g) are present in the condensed phase at 190 °C and rising up to the maximum gradually.

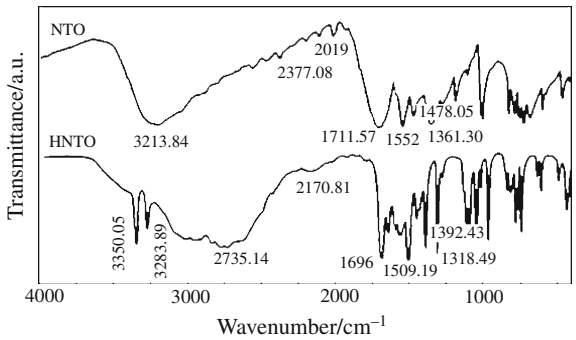

Fig. 3 FTIR spectra of HNTO

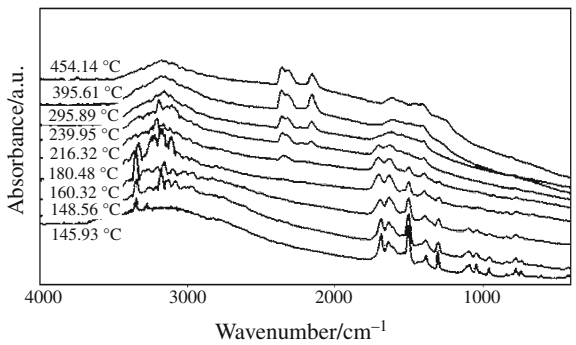

Fig. 4 IR spectra of the condensed phase decomposition products of HNTO at various temperatures

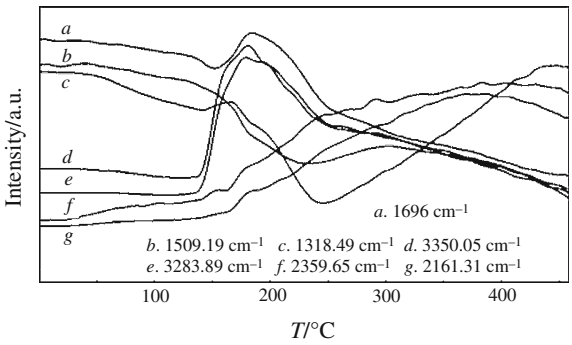

Fig. 5 IR characteristic absorption peak intensity curves of the condensed phase decomposition products of HNTO

It is obvious that the decomposition process of HNTO can be expressed as: nitryl group break first away from HNTO molecule, then hydrazine group break almost simultaneously away with carbonyl group, accompanying azole ring breaking in the main exothermic reaction process (stage I); and the reciprocity of fragments generated from the decomposition reaction is appeared in the second one (stage II).

Total energy, frontier orbital energy (Hartree), and the percentage of orbital compositions of the compound

According to the selected basic set and molecule structure, there are 101 molecule orbits in this system including 42 occupied ones. Molecular total energies, frontier orbital energy levels, their gaps, and the atomic orbital compositions in HOMO and LUMO are listed in Table 1.

According to the MO theory, HOMO and LUMO are the most important factors that affect the property of the compound. HOMO has the priority to provide electrons, while LUMO can accept electrons first [21, 27]. Thus, the study on the frontier orbital energy can provide valuable information about the active mechanism.

Taking B3LYP result, for example, from MO results (Table 1), the main compositions are atom N1, N2, C3, N4, O6 in HOMO, and atom N2, N7, O8, O9 in LUMO. The HOMO orbits are consisted of *p* orbit of N1, N2, C3, N4, and O6 atoms in triazole ring, and the LUMO orbits are consisted of *p* orbit of N2, N7, O8, and O9 atoms. This HOMO condition also shows that the conjugation of the triazole ring is concerned mainly with N1, N2, C3, N4, and O6; and N, O atoms in the nitryl do not contribute to the conjugation. The electron density in HOMO and LUMO is shown in Fig. 6. As the property is to be related to frontier

Table 1 Total energy, frontier orbital energy (Hartree), and the percentage of orbital compositions of the compound

E_{total}				−633.877632870
E_{HOMO}				−0.24210
E_{LUMO}				−0.09250
ΔE^a				0.1496
Atoms	HOMO		LUMO	
	s^b	p^b	s^b	p^b
N1	–	13.45	–	4.33
N2	–	21.78	–	11.32
C3	–	8.39	–	2.87
N4	–	15.15	–	2.73
C5	–	5.15	–	–
O6	–	29.46	–	–
N7	–	–	–	35.02
O8	–	2.71	–	20.29
O9	–	–	–	20.26
N11	1.01	–	1.18	–
N12	1.22	–	–	–

[a] $\Delta E = E_{LUMO} - E_{HOMO}$

[b] s and *p* represent *s* and *p* orbits, respectively

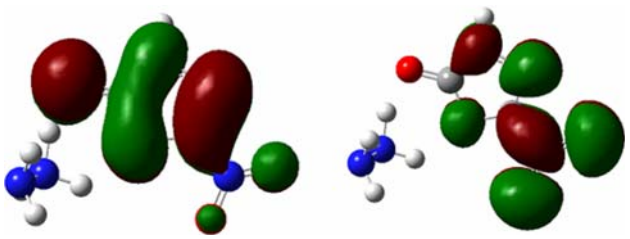

Fig. 6 View of HOMO (*left*) and LUMO (*right*) for the title compound by B3LYP method

orbit, some properties of the title compound is decided by NTO.

Condensation to atoms

From Table 2, one can see that C3 and N7 are the weakest antibonding molecule orbits (AMO) in NTO ring. The C–N bond strength sequence in the NTO pentabasic ring can be obtained from Table 2 as: C3–N4 > N2–C3 > N4–C5 > N1–C5. Table 2 also shows that the weakest bond in NTO^- is N7–C3 (−0.051002). Generally speaking, this bond will be broken preferentially and nitryl is easier to be dissociated when NTO (or HNTO) is decomposed, which is in agreement with the thermal decomposition mechanism of other complexes derived from NTO [28].

Therefore, it can be concluded that when the title compound is heated to a certain temperature, N7–C3 bond will break first from HNTO molecule, then N1–C5, N4–C5, and N11–N4 break simultaneously. The result is in agreement with that of the thermal decomposition experiment.

Table 2 Condensation to atoms

Bonds	B3LYP
N1–N2	−0.227281
N1–C5	0.051957
N2–C3	0.295943
C3–N4	0.368011
C5–O6	0.181542
N4–C5	0.204631
N7–C3	−0.051002
N7–O8	0.405663
N7–O9	0.377170
N11–N4	−0.228053
N12–N11	−0.446658

Conclusions

The thermal decomposition mechanism of hydrazine HNTO was studied by the experiment investigation and the quantum chemical calculation. HNTO has two exothermic decomposition reaction stages: nitryl group break first away from HNTO molecule, then hydrazine group break almost simultaneously away with carbonyl group, accompanying azole ring breaking in the first stage; and the reciprocity of fragments generated from the decomposition reaction is appeared in the second one. The C–N bond strength sequence in the pentabasic ring can be obtained from the quantum chemical calculation as: C3–N4 > N2–C3 > N4–C5 > N1–C5. The weakest bond in NTO^- is N7–C3. N11–N4 bond strength is almost equal to N4–C5. The theoretic calculation is in agreement with that of the thermal decomposition experiment. The decomposition mechanism of HNTO is in agreement with the thermal decomposition mechanism of other complexes derived from NTO.

Acknowledgements We acknowledge the support of the National Natural Science Foundation of China (No. 20573098) and the Foundation of National Key Laboratory of Science and Technology on Combustion (No. 9140C3503020605).

References

1. Lee KY, Chapman LB, Coburn MD. A less sensitive explosive: 3-nitro-1,2,4-triazol-5-one. J Energy Mater. 1987;5:27–33.
2. Lee KY, Coburn MD. 3-Nitro-1,2,4-triazol-5-one, a less sensitive explosive. USP 4,733,610. 1988.

3. Zhang TL. Study on preparation, structure characterization, decomposition mechanism and nonisothermal reaction kinetics of NTO. PhD Dissertation, Nanjing University of Science & Technology, Nanjing, 1993.
4. Song JR. Study on NTO–metal complex. Beijing: Chemical Industry Press; 1998.
5. Li JR, Chen BR, Ou YX, Fan GY, Cui XS. The crystal structure of lead 3-nitro-1,2,4-triazol-5-one (NTO). J Beijing Inst Technol. 1993;13:157–60.
6. Li JR, Chen BR, Ou YX, Zhu NJ. Crystal structure of ammonium 3-nitro-1,2,4-triazol-5-onate. Propellants Explos Pyrotech. 1991;16:145–6.
7. Zhang TL, Hu RZ, Li FP, Chen L. Preparation, molecular structure and thermal decomposition mechanism of $[Cu(NTO)_2(H_2O)_2]\cdot 2H_2O$. Chin Sci Bull. 1993;38:1350–3.
8. Zhang TL, Hu RZ, Li FP. Structural characterization and thermal decomposition mechanisms of alkaline earth metal (Mg, Ca, Sr, and Ba) salts of 3-nitro-1,2,4-triazol-5-one. Thermochim Acta. 1984;244:185–94.
9. Xie Y, Hu RZ, Zhang TL, Li FP. Studies on the synthesis and thermal decomposition mechanisms of rare-earth metal (Pr, Nd, Sm) salt hydrates of 3-nitro-1,2,4-triazol-5-one. J Therm Anal. 1993;39:41–5.
10. Zhang TL, Hu RZ, Li FP. Preparation, structure characterization and thermal decomposition mechanism of rare salts of 3-nitro-1,2,4-triazol-5-one. J Rare Earths. 1995;13:10–5.
11. Hu RZ, Song JR, Li FP, Kang B, Kong YH, Mao ZH, et al. Preparation, crystal structure, thermal decomposition mechanism and thermodynamical properties of $[Dy(NTO)_2(H_2O)_6]NTO\cdot 4H_2O$. Thermochim Acta. 1997;299:87–93.
12. Song JR, Hu RZ, Li FP, Zhang TL, Mao ZH, Zhou ZH, et al. Preparation, crystal structure and thermal decomposition mechanism of $[Co(H_2O)6](NTO)_2\cdot 2H_2O$. Chin Sci Bull. 1996;41:1806–10.
13. Song JR, Hu RZ, Kang B, Li FP. Preparation, crystal structure, thermal decomposition mechanism and thermodynamical prosperites of $[Yb(NTO)_3(H_2O)_4]\cdot 6H_2O$ and $[Sr(NTO)_2(H_2O)_4]_2\cdot 4H_2O$. Thermochim Acta. 1999;331:49–60.
14. Song JR, Hu RZ, Kang B, Li FP. Preparation, crystal structure, thermal decomposition mechanism, and thermodynamical properties of $H[Pr(NTO)_4(H_2O)_4]\cdot 2H_2O$.Thermochim Acta. 1999;335:19–25.
15. Song JR, Ning BK, Hu RZ, Kang B. Preparation, crystal structure and thermal decoruposition process of $[Y(NTO)_2NO_3(H_2O)_5]\cdot 2H_2O$.Thermochim Acta. 2000;352–353:111–5.
16. Yang L, Zhang TL, Feng CG, Yu KB. Preparation and molecular structure of AGNTO. Acta Phys Chim Sin. 2001;17:438–42.
17. Singh G, Kapoor IPS, Mannan SM, Tiwari SK. Studies on energetic compounds part 7: thermolysis of ring substituted arylammonium salts of 3-nitro-1,2,4-triazole-5-one (NTO). J Energy Mater. 1998;16:101–8.
18. Singh G, Felix SP. Studies of energetic compounds, part 29: effect of NTO and its salts on the combustion and condensed phase thermolysis of composite solid propellants, HTPB-AP. Combust Flame. 2003;132:422–32.
19. Singh G, Felix SP. Studies on energetic compounds. Part 32: crystal structure, thermolysis and applications of NTO and its salts. J Mol Struct. 2003;649:71–83.
20. Singh G, Felix SP. Studies on energetic compounds 25: an overview of preparation, thermolysis and applications of the salts of 5-nitro-2,4-dihydro-3H-1,2,4-triazol-3-one (NTO). J Hazard Mater. 2002;A90:1–17.
21. Ma HX, Song JR, Hu RZ, Li J. Non-isothermal kinetics of the thermal decomposition of 3-nitro-1,2,4-triazol-5-one magnesium complex. Chin J Chem. 2003;21:1558–61.
22. Yi JH, Zhao FQ, Gao HX, Xu SY, Wang MC, Hu RZ. Preparation, characterization, nonisothermal reaction kinetics, thermodynamic properties, and safety performances of high nitrogen compound: hydrazine 3-nitro-1,2,4-triazol-5-one complex. J Hazard Mater. 2008;153:261–8.
23. Wu KW, Hou HY, Shu CM. Thermal phenomena studies for dicumyl peroxide at various concentrations by DSC. J Therm Anal Calorim. 2006;83:41–4.
24. Yi JH, Zhao FQ, Xu SY, Zhang LY, Ren XN, Gao HX, et al. Effect of pressures on decomposition reaction kinetics of double-base propellant catalyzed with cerium citrate. J Therm Anal Calorim. 2009;95:381–5.
25. Li JZ, Fan XZ, Hu RZ, Zheng XD, Zhao FQ, Gao HX. Thermal behavior of copper(II) 4-nitroimidazolate. J Therm Anal Calorim. 2009;96:195–201.
26. Frisch MJ, Trucks GW, Schlegel HB, Scuseria GE, Robb MA, Cheeseman JR, et al. Gaussian 03, Revision B. 01. Pittsburgh, PA: Gaussian Inc.; 2003.
27. Ma HX, Song JR, Xu KZ, Hu RZ, Zhai GH, Wen ZY, et al. Preparation, crystal structure and theoretical calculation of $(CH_3)_2NH_2^+ C_2N_4OH^-$. Acta Chim Sin. 2003;61:1819–23.
28. Ma HX, Song JR, Xu KZ, Hu RZ, Wen ZY. The thermal decomposition mechanism and the quantum chemical calculation of $[Mg(H_2O)_6](NTO)_2\cdot 2H_2O$. Chin J Energy Mater. 2004;12:158–60, 164.